AIAA JOURNAL
Vol. 32, No. 3, March 1994

Stochastic Approach to Noise Modeling for Free Turbulent Flows

Walid Béchara,* Christophe Bailly,† and Philippe Lafon‡
Electricité de France, Direction des Etudes et Recherches, 92141 Clamart, France
and
Sébastien M. Candel§
Ecole Centrale Paris, 92295 Châtenay-Malabr, France

A new approach to noise modeling for free turbulent flows is presented. The equations governing the sound field are obtained in two steps. The first step consists of treating the mean and turbulent components of the flow while the acoustic perturbations are neglected. In the second step, a set of equations is derived for the acoustic variables. On the left-hand side of this system, one finds the linearized Euler equations, whereas the right-hand side exhibits source terms related to the turbulent fluctuations and their interactions with the mean flow. These terms are modeled using a stochastic description of the three-dimensional turbulent motion. This is achieved by synthesizing the velocity field at each point in space and for all times with a collection of discrete Fourier modes. The synthesized field posesses the suitable one- and two-point statistical moments and a reasonable temporal power spectral density. The linearized Euler equations including a stochastic description of noise sources are solved numerically with a scheme based on a fractional step treatment. Each one-dimensional problem is solved with a weak formulation. A set of calculations are carried out for a simple freejet. Comparisons between calculations and experiments indicate that a spatial filtering of the source terms is required to obtain the expected level in the far field. Realistic pressure signals, power spectral densities, and sound field patterns are obtained. It is indicated that the stochastic noise generation and radiation (SNGR) approach may be applied to more complex flows because the numerical codes used to calculate the mean flowfield and the wave propagation are not specific of jet configurations. The limitations of the present model lie in the statistical properties of the synthetic turbulent field and in the use of an axisymmetric modeling of the acoustic propagation.

I. Introduction

LIGHTHILL'S theory[1] of acoustic radiation from a limited volume of turbulent fluid embedded in an infinite homogeneous medium at rest uses an analogy between the acoustic fluctuations generated by the turbulent perturbations and the acoustic fluctuations which result from a quadrupole distribution of strength T_{ij} in a fictitious equivalent domain at rest. The source term T_{ij} contains the instantaneous Reynolds stress tensor $\rho u_i u_j$ of the turbulence and, if there is a mean flow as in a jet, a cross product term of mean flow and turbulence.[2-6] Because the governing wave equation is so simple, the instantaneous sound pressure at a point may be expressed as an integral in terms of T_{ij} in retarded time over the source region. But the T_{ij} tensor is stochastic and can normally be defined only in a statistical sense. This leads to the determination of mean square sound pressure in terms of a double integral of two point space-time correlations of T_{ij} (Refs. 2-8).

Using assumed correlations in an approximate form of T_{ij} (Ref. 9), (variants of this procedure), Ribner,[3] Pao and Lowson,[10] and Goldstein and Rosenbaum[7] found predictions of jet noise directivity in good agreement with those obtained in the experiment. Closely related to this approach, we have also tried to bring the modeling a step further by determining all of the local properties of the noise source terms from a numerical solution of the mean flow equations coupled with a turbulence closure model.[11,12] A single adjustable factor remains in the formulation which may be determined once. It is then shown in Refs. 11 and 12 that the model has predictive capabilities and may be used to study different jet configurations. The good results obtained demonstrate the value of the Ribner and Goldstein models.

Over the years different methods have been devised to directly include the flow effects of sound propagation (and also its generation). In the development due to Phillips,[13] the Lighthill equation is replaced by an inhomogeneous wave equation for a moving medium with the flow effects appearing in the wave operator rather than in the T_{ij} source term. Mani[14] obtained comparably good agreement by, in effect, moving part of T_{ij} to the left-hand (operator) side of the Lighthill wave equation. This equation was modified by Lilley[15] to further separate propagation terms and source terms. Much work has been expended to solve Lilley's equation for uniform and nonuniform mean flows. Analytic solutions have been proposed for the high-frequency range[8,16-18] and for the low-frequency propagation.[8,14,16,19,20] Numerical calculations of the three-dimensional axisymmetric refraction of sound waves by jet flows were performed by Schubert[21,22] whereas three-dimensional refraction effects were studied by Candel[23] using geometrical methods. Exact numerical solutions of source radiation in shear flows were obtained with Fourier methods by Candel and Crance.[24]

In general, these studies deal with the propagation of acoustic waves due to monopolar or quadrupolar source points. The analytical solutions derived are rather sophisticated and lack generality. The sound generation models are also rather specialized. Being analytically and numerically much more difficult to apply than the Lighthill-based formalisms, the added labor has not yet paid off in predictive capability.

Received June 15, 1992; revision received May 17, 1993; accepted for publication June 9, 1993.

*Ph.D. Candidate, Department Acoustique et Mécanique Vibratoire, 1 avenue du G. de Gaulle; currently Research Engineer, Centre de Recherches Claude Delorme de l'Air liquide, BP 126, 78350 Les Loges en Josas, France.

†Ph.D. Candidate, Department Acoustique et Mécanique Vibratoire, 1 avenue du G. de Gaulle.

‡Research Engineer, Department Acoustique et Mécanique Vibratoire, 1 avenue du G. de Gaulle. Member AIAA.

§Professor of Fluid Mechanics, Lab. EM2C, CNRS. Member AIAA.

However, the work done on this problem has enhanced the current understanding of aerodynamic noise generation and propagation.

A possible advance has been explored by Berman and Ramos.[25] It consists of numerically solving a third-order Lilley's equation transformed into a system of first-order, time-dependent partial differential equations. Numerical results from a K-ϵ turbulence code are used to determine the velocity field of the mean flow and to simulate the turbulent fluctuation involved in the source term. The numerical solution is effected for one test case with an overly simplified description of turbulence, and the validations presented in his paper are insufficient, but the idea merits further attention.

The present article explores a novel approach to noise modeling for free turbulent flows. In essence, we are going to derive a system of first-order equations describing the propagation of the acoustic field and containing the source terms related to the turbulent fluctuations. These terms are modeled using a stochastic description of the three-dimensional turbulent motion. A stochastic noise generation and radiation (SNGR) model is derived on this basis. The noise source terms are defined by synthesizing the velocity field at each point in the flow with a discrete set of Fourier modes. The synthetic turbulent field possesses the proper one- and two-point statistical spatial moments and an acceptable temporal spectral density. In practice the flowfield is subdivided in a collection of independent source regions with longitudinal and lateral dimensions defined by the local correlation scales of turbulence. Although this synthetic representation has many of the characteristics of real turbulence, it is not perfect. It exhibits the expected correlation lengths and, in particular, the required ratio of length scales but does not feature the convective properties of shear flow turbulence. Under these circumstances one cannot expect to obtain a definitive model for aerodynamic noise radiation. In particular, the convective amplification that is typical of the radiation process when the sources are convected at high speed will be missing from the model. This effect was not included in this first attempt at stochastic modeling of the noise generation process because it would have required a much more complex numerical implementation. Although we are aware of the limitations of the model, we also note that it is worth exploring the SNGR concept even with some simplifications and later proceeding with a full implementation. Another limitation of the present study lies in the propagation step. In principle, a three-dimensional computational method would be needed to propagate acoustic waves from the noise sources. This would require a very large grid and unacceptable computational loads. For these reasons, it was decided that an axisymmetric propagation scheme would be used to calculate the radiated field. This choice reduces the calculation to a two-dimensional problem and allows a description of refraction effects. It also has an influence on the spatial radiation of acoustic waves from the noise sources. The related error is accepted in the present study because we wish to test the concept but improvements of this aspect will also be needed in future studies.

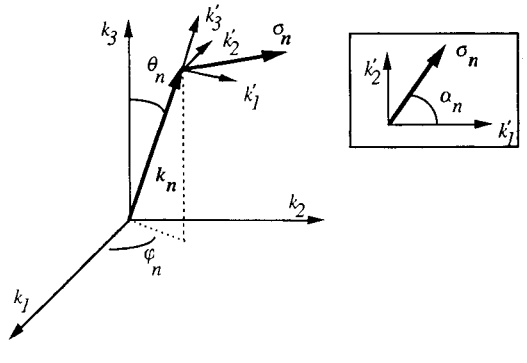

Fig. 1 Wave vector geometry for the nth Fourier velocity mode; the unit vector σ_n lies in the (k_1', k_2') plane perpendicular to k_n and its polar angle α_n has an arbitrary orientation.

Finally, as in most aeroacoustic studies, we neglect the viscous sources which are believed to be less important at high Reynolds numbers, and we also use the linearized approximation, which is not completely justified. Indeed, amplitudes may be quite high in the vicinity of the sound emitting volume, but the linear treatment is commonly used in practice.

We begin by establishing the basic equations of the SNGR model (Sec. II). In Sec. III we show how one may synthesize a turbulent flowfield using stochastic principles. The statistical characteristics of the flow are first determined with a K-ϵ turbulence model and used to scale the simulated fluctuations. Section IV describes the different steps of a typical calculation. The simple case of a turbulent freejet is treated as an example in Sec. V, which also contains comparisons between calculations and experiments of Lush.[26]

II. Basic Formulation of the Stochastic Noise Generation and Radiation Model

Although the tendency has been to set noise problems in terms of second-order or even higher order wave equations (of which Lilley's equation is typical), this is not appropriate for a numerical solution. In fact, it is more adequate to use a formulation in terms of first-order partial differential equations. It is of course possible to start from a third-order equation and go back to a first-order system as was done by Berman and Ramos,[25] but it is more natural to start directly from the basic equations of fluid mechanics.

Let us now consider the generation of noise by a stationary turbulent flowfield. One may distinguish mean, turbulent, and acoustic components in each flow variable (pressure p, velocity u_i, and density ρ) and write these variables as follows:

$$\begin{aligned} p &= P + p_t + p_a \\ u_i &= U_i + u_{ti} + u_{ai} \\ \rho &= \bar{\rho} + \rho_t + \rho_a \end{aligned} \tag{1}$$

In general, the acoustic fluctuations are small compared to the mean and turbulent variables, so that one may assume that the following relations are satisfied:

$$\begin{aligned} &p_a/p_t << 1, \quad u_{ai}/u_{ti} << 1, \quad \rho_a/\rho_t << 1 \\ &p_a/P << 1, \quad u_{ai}/U_i << 1, \quad \rho_a/\bar{\rho} << 1 \end{aligned} \tag{2}$$

One may then formulate the governing equations for the acoustic variables by proceeding in two steps.

In the first step one considers the evolution of the mean and turbulent components of the flow by neglecting the acoustic perturbations. This step is similar to the classical Reynolds decomposition of turbulent flows. Because we are interested in noise radiated by subsonic flows, it is reasonable to assume that the mean density is constant and the density fluctuations are negligible ($\rho_t \simeq 0$). The Reynolds averaged equations of motion are:

$$\frac{\partial U_i}{\partial y_i} = 0 \tag{3}$$

$$\bar{\rho} U_j \frac{\partial U_i}{\partial y_j} + \frac{\partial P}{\partial y_i} + \bar{\rho} \frac{\partial \overline{u_{ti} u_{tj}}}{\partial y_j} = 0 \tag{4}$$

Note that the turbulent velocity u_{ti} is also divergence-free: $\partial u_{ti}/\partial y_i = 0$. In the system of equations (3) and (4), the viscous terms may be neglected because the viscous stresses are much smaller than the Reynolds stresses in free-shear flows. Of course, the viscous dissipation is retained in the turbulence closure model which is added to Eqs. (3) and (4) to determine the Reynolds stresses. On the other hand, if we limit the analysis to the case of turbulent flow at ambient temperature, the heat generated by the viscous dissipation may be neglected

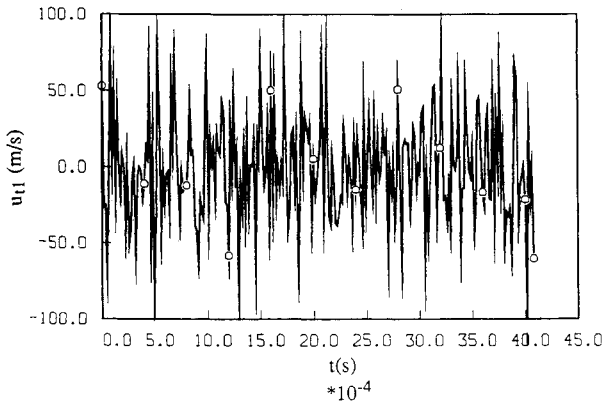

a) ○, time evolution of the signal u_{t1}

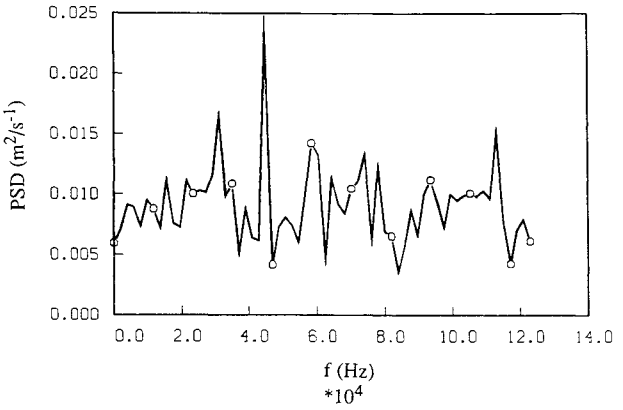

b) ○, power spectral density of u_{t1}; the averaging is performed over 23 periodograms of 128 samples

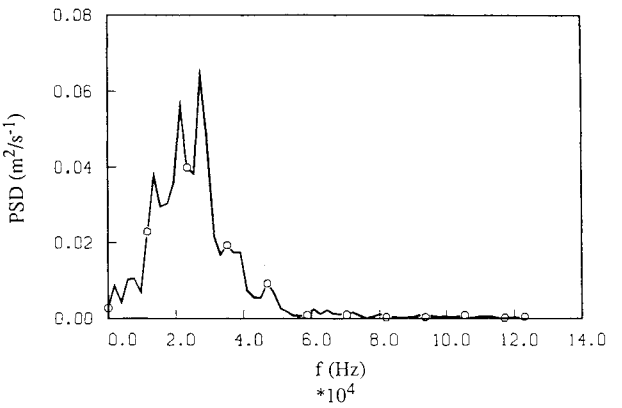

c) ○, power spectral density of the signal after convolution with a finite impulse response filter; the averaging is performed over 23 periodograms of 128 samples

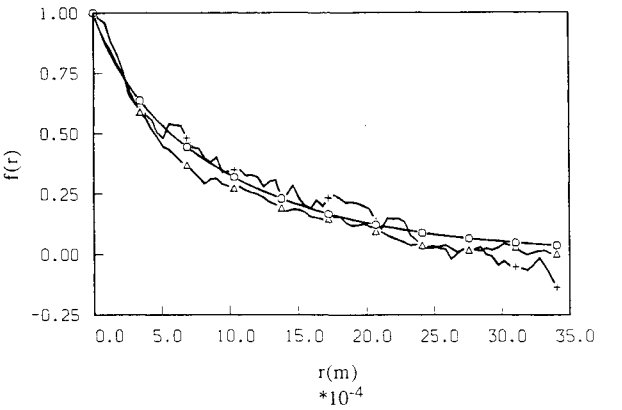

d) Variation of the longitudinal correlation function $f(r)$ with the distance variable: ○, theoretical; Δ, simulated before convolution and +, simulated after convolution

Fig. 2 Simulated turbulent velocity u_{t1} before and after filtering.

and the isentropic flow assumption is reasonable in the subsonic range. Under these conditions, we can rewrite the continuity equation in terms of pressure and velocity variables. Substituting $p = P + p_t$ and $u_i = U_i + u_{ti}$, and averaging the resulting equation, one obtains:

$$U_i \frac{\partial P}{\partial y_i} + \gamma \overline{p_t \frac{\partial u_{ti}}{\partial y_i}} + \overline{u_{ti} \frac{\partial p_t}{\partial y_i}} = 0 \tag{5}$$

where we have used the relation $(\partial p/\partial \rho)_s = \gamma p/\rho$ for an ideal gas where γ represents the ratio of the specific heats at constant pressure and volume.

In the second step we consider the acoustic component and assume that mean and turbulent components of the flow are known. It is convenient to start from Euler's system in which the continuity equation is also written in terms of pressure and velocity variables:

$$\frac{\partial p}{\partial t} + \gamma p \frac{\partial u_i}{\partial y_i} + u_i \frac{\partial p}{\partial y_i} = 0 \tag{6}$$

$$\frac{\partial u_i}{\partial t} + u_j \frac{\partial u_i}{\partial y_j} + \frac{1}{\rho} \frac{\partial p}{\partial y_i} = 0 \tag{7}$$

Inserting the decomposition of variables (1), neglecting the turbulent density fluctuations $\rho_t \approx 0$, and considering that the acoustic perturbations are isentropic $p_a = c^2 \rho_a$ in Eqs. (3-5), one finds:

$$\frac{\partial p_a}{\partial t} + U_i \frac{\partial p_a}{\partial y_i} + \gamma P \frac{\partial u_{ai}}{\partial y_i} + \gamma p_a \frac{\partial U_i}{\partial y_i} + \overline{u_{ai} \frac{\partial P}{\partial y_i}}$$

$$= -\frac{\partial p_t}{\partial t} - U_i \frac{\partial p_t}{\partial y_i} - u_{ti} \frac{\partial P}{\partial y_i} - \overline{u_{ti} \frac{\partial p_t}{\partial y_i}} + \overline{u_{ti} \frac{\partial p_t}{\partial y_i}} \tag{8}$$

$$\frac{\partial u_{ai}}{\partial t} + U_j \frac{\partial u_{ai}}{\partial y_j} + \frac{1}{\bar{\rho}} \frac{\partial p_a}{\partial y_i} + u_{aj} \frac{\partial U_i}{\partial y_j} - \frac{p_a}{\bar{\rho}^2 \bar{c}^2} \frac{\partial P}{\partial y_i}$$

$$= -U_j \frac{\partial u_{ti}}{\partial y_j} - u_{tj} \frac{\partial U_i}{\partial y_j} - \overline{u_{tj} \frac{\partial u_{ti}}{\partial y_j}} - \frac{1}{\bar{\rho}} \frac{\partial p_t}{\partial y_i} - \frac{\partial u_{ti}}{\partial t} + \frac{\partial}{\partial y_j} \overline{u_{tj} u_{ti}} \tag{9}$$

In Eq. (8), the term $\gamma p_a \partial U_i/\partial y_i$ is retained to obtain a set of expressions (8) and (9) featuring a left-hand side which is identical to the linearized Euler equations.[8] This is purely formal as the divergence of U_i vanishes according to Eq. (3). To simplify the analysis, terms describing effects of turbulence-acoustic interactions and of nonlinear acoustics are neglected.

The right-hand side of system (8) and (9) exhibits the source terms responsible for the noise generation. The identification of the principal terms which contribute to the noise emission is not a simple matter. However, we know from previous works[2,3] that the main sources of sound generated by turbulence are the first terms of the right-hand side of Eq. (9). This reasoning based on previous knowledge is essentially confirmed by an order of magnitude analysis. In particular, the first two terms represent the interaction between the mean and turbulent components of the flow. The third term represents turbulence-turbulence interactions. The noise associated with the first two terms is usually called shear noise whereas that due to the third term is denoted as self noise. These three terms are the main sources of the sound generated aerodynamically

and one may neglect the other contributions. After simplification, the system of equations becomes

$$\frac{\partial p_a}{\partial t} + U_i\frac{\partial p_a}{\partial y_i} + \gamma P\frac{\partial u_{ai}}{\partial y_i} + \gamma p_a\frac{\partial U_i}{\partial y_i} + u_{ai}\frac{\partial P}{\partial y_i} = 0 \tag{10}$$

$$\frac{\partial u_{ai}}{\partial t} + U_j\frac{\partial u_{ai}}{\partial y_j} + \frac{1}{\bar\rho}\frac{\partial p_a}{\partial y_i} + u_{aj}\frac{\partial U_i}{\partial y_j} - \frac{p_a}{\bar\rho^2\bar c^2}\frac{\partial P}{\partial y_i} = -U_j\frac{\partial u_{ti}}{\partial y_j} - u_{tj}\frac{\partial U_i}{\partial y_j} - u_{tj}\frac{\partial u_{ti}}{\partial y_j} \tag{11}$$

To estimate the source terms it is necessary to calculate the mean flow and simulate a space-time turbulent velocity field. For this we use a standard K-ϵ code that supplies mean quantities and second-order moments, in combination with a stochastic method providing the space-time turbulent velocity fluctuations. The determination of this field is described in the next section.

III. Stochastic Simulation of a Turbulent Velocity Field

The spatial velocity field is synthesized with a method devised by Kraichnan[27] and improved by Karweit et al.[28,29] In this method, one generates a random velocity field which is defined as a finite sum of discrete Fourier modes. This turbulent three-dimensional field is isotropic and homogeneous and considered to be frozen. The method provides a random velocity field having the proper spatial characteristics. It has been used in the past to study the behavior of acoustic waves propagating through a turbulent medium. We use this same approach for simulating a turbulent velocity field having the turbulent kinetic K energy and the dissipation rate ϵ obtained from a standard K-ϵ code. In addition, it is necessary to deduce a time series from the stochastic velocity field. This item will be described later.

Consider first a three-dimensional Fourier decomposition of a turbulent homogeneous isotropic field at given point $\boldsymbol{y}$

$$u_t(\boldsymbol{y}) = \int \tilde u_t(\boldsymbol{k}) e^{j\boldsymbol{k}\cdot\boldsymbol{y}}\,\mathrm{d}\boldsymbol{k} \tag{12}$$

where $\boldsymbol{k}$ is the wave vector and j is the complex number ($j^2 = -1$). By transforming this Fourier integral into a limited sum of N modes, one may write

$$u_t(\boldsymbol{y}) = 2\sum_{n=1}^{N} \tilde u_{tn}\cos(\boldsymbol{k}_n\cdot\boldsymbol{y} + \Psi_n)\boldsymbol{\sigma}_n \tag{13}$$

where $\tilde u_{tn}, \Psi_n$, and $\boldsymbol{\sigma}_n$ are the amplitude, phase, and the direction of the nth mode associated with the wave vector $\boldsymbol{k}_n$. Moreover, for an incompressible turbulent field, the relation $\partial u_{ti}/\partial y_i = 0$ requires that

$$\boldsymbol{k}_n\cdot\boldsymbol{\sigma}_n = 0, \qquad n = 1,\ldots,N \tag{14}$$

This indicates that in the spectral space, the unit vector $\boldsymbol{\sigma}_n$ is always perpendicular to the wave vector $\boldsymbol{k}_n$ and its position is determined by its polar angle α_n (see Fig. 1). The wave vector $\boldsymbol{k}_n$ may be characterized by its spherical coordinates (k_n, φ_n, θ_n). The isotropic and homogeneous random field is obtained by choosing probability density functions for the random variables φ_n, θ_n, Ψ_n, and α_n. It may be shown that $P(\varphi_n)$, $P(\alpha_n)$, and $P(\Psi_n)$ should be uniform densities: $P(\varphi_n) = P(\alpha_n) = \frac{1}{2}\pi$, and $P(\Psi_n) = 1/\pi$. On the other hand, the distribution of θ_n is given by a sine function: $P(\theta_n) = \frac{1}{2}\sin\theta_n$.

For a complete description of the field (13), one has to determine the amplitude $\tilde u_{tn}$ for each Fourier mode. The statistical mean (noted $<>$) of $\frac{1}{2}u_{ti}u_{ti}$ is the turbulent kinetic energy K, and according to Eq. (13), this quantity takes the form

$$K = \sum_{n=1}^{N} \tilde u_{tn}^2 \tag{15}$$

An homogeneous isotropic turbulence is characterized by a three-dimensional spectrum $E(k)$ (Ref. 30) which is such that

$$\int_0^\infty E(k)\,\mathrm{d}k = K \tag{16}$$

$$2\nu\int_0^\infty k^2E(k)\,\mathrm{d}k = \epsilon \tag{17}$$

The amplitude $\tilde u_{tn}$ of each mode is equal to $\sqrt{E(k_n)\Delta k_n}$, and one uses the modified Von Karman spectrum $E(k)$ to simulate the complete spectral range:

$$E(k) = A\frac{\frac{2}{3}K}{k_e}\frac{(k/k_e)^4}{[1+(k/k_e)^2]^{17/6}}\exp[-2(k/k_{\mathrm{Kol}})^2] \tag{18}$$

The two parameters A and k_e are determined from relations (16) and (17), whereas k_{Kol} is the Kolmogorov wave number defined by $(\epsilon/\nu^3)^{1/4}$. The spectrum reaches its maximum for k_e.

To assign the spectral power to a finite number of N modes, it is adequate to use a logarithmic distribution of the N wave numbers. This provides a better discretization of the power in the lower wave number range corresponding to the larger, energy-containing eddies. The logarithmic step Δk_l of this distribution is given by

$$\Delta k_l = \frac{\log k_N - \log k_1}{N-1} \tag{19}$$

and

$$k_n = \exp[\log k_1 + (n-1)\log\Delta k_l] \tag{20}$$

The wave number $k_l = 2\pi/L$ corresponds to the largest eddy (L is the largest eddy scale), whereas $k_N = (\epsilon/\nu^3)^{1/4} = k_{\mathrm{Kol}}$ designates the Kolmogorov wave number.

One has to verify that this procedure yields a turbulent field featuring the required one-point first-, second-, and third-order statistical moments. For an isotropic homogenous turbulence the following equalities apply:

$$\begin{aligned} &<u_{t1}> = <u_{t2}> = <u_{t3}> = 0\\ &<u_{t1}^2> = <u_{t2}^2> = <u_{t3}^2> = \tfrac{2}{3}K\\ &<u_{t1}^3> = <u_{t2}^3> = <u_{t3}^3> = 0\\ &<u_{t1}u_{t2}> = <u_{t2}u_{t3}> = <u_{t1}u_{t3}> = 0 \end{aligned} \tag{21}$$

As the mode number N is increased and as the number of samples N_r is augmented, the difference between theory and simulation diminishes. With N fixed to 200 Fourier modes and $N_r = 1000$, the simulation is quite satisfactory.[12] In addition, one wishes to obtain the correct longitudinal and lateral correlation functions $f(r)$ and $g(r)$. Using the spectrum $E(k)$ for an isotropic homogeneous turbulence, one can determine an analytic expression for $f(r)$ and $g(r)$ (see Ref. 30). On the other hand, it is known from an analysis of the two points correlation tensor, that $f(r)$ is equal to $<u_{t1}(0,0,0)u_{t1}(r,0,0)>/<u_{t1}^2(0,0,0)>$, and $g(r)$ is equal to $<u_{t2}(0,0,0)u_{t2}(r,0,0)>/<u_{t2}^2(0,0,0)>$. These identities are verified in Ref. 12.

In a first step, one calculates a collection of spatial turbulent fields without temporal correlation. At given point in space, one may then consider that each independent realization provides a velocity sample. The successive samples may be used to form a time series. A typical sequence of samples is displayed in Fig. 2a for one turbulent component u_{t1} (here, the mean velocity is equal to $U_1 = 300$ m/s and the local kinetic energy is equal to 1714 m^2/s^2). The velocity fluctuations are of the order of $0.17U_1$. The power spectral density of this signal represented in Fig. 2b is that of a white noise because each sample in the time series is independent. However, the real

turbulent signal is characterized by a dominant frequency that is modeled by ϵ/K. The correct temporal correlation of the turbulent velocity signal is obtained through filtering in the frequency domain. The initial time series is bandpass filtered with a linear phase finite impulse response filter, having a transfer function which may be described by a Gaussian entered on the frequency $f_0 = \epsilon/K$ ($|\tilde{H}(f)| = \exp[-(f-f_0)^2/a^2 f_0^2]$ where $f_0 = 26$ kHz and $a = \frac{1}{2}$ in the example shown in Fig. 2. The convolution of the signal u_{t1} with the inverse Fourier transform of $\tilde{H}(f)$ yields a suitable temporal signal as indicated by Fig. 2c which displays the power spectral density of the filter output signal. The power distribution is now centered on the frequency ϵ/K, and it has a finite bandwidth.

As indicated in the Introduction, the present process of noise source generation does not account for the convection effects that are found in typical shear flows. Consequently, we expect that the convective amplification that characterizes moving sources will not be retrieved. However, effects of the flow on the propagation from the sources will be well described in the computation. Although this is a definite weakness of the present model, it may be corrected in future studies by applying a more elaborate stochastic synthesis method.

IV. Application of the Stochastic Noise Generation and Radiation Model

The successive steps in applying the model are now described in the six following points.

1) An aerodynamic flowfield calculation is first carried out to determine the mean and turbulent quantities of the flow. The equations solved in this step are the Reynolds-averaged Navier-Stokes equations, and the turbulence closure is the K-ϵ model. We use the Ulysse code, developed in the Laboratoire National d'Hydraulique of the Direction des Etudes et Recherches d'Electricité de France.[31]

2) The turbulent region which contributes to the acoustic emission is identified in the second step. In theory all of the flowfield contributes to the acoustic emission. However, if one examines the local acoustic power, one finds that for a free turbulent jet,[11] the source domain may be limited to the initial mixing layer and the transition region.

3) The source domain is divided into a finite number of uncorrelated regions. The subdivision of the source region is based on the local correlation scales l_1 and l_2

$$l_1 = \overline{u_{t1}^2}^{3/2}/\epsilon; \qquad l_2 = \overline{u_{t2}^2}^{3/2}/\epsilon \tag{22a}$$

where

$$\overline{u_{t1}^2} = -2\nu_t \partial U_1/\partial y_1 + \tfrac{2}{3}K; \quad \overline{u_{t2}^2} = -2\nu_t \partial U_2/\partial y_2 + \tfrac{2}{3}K \tag{22b}$$

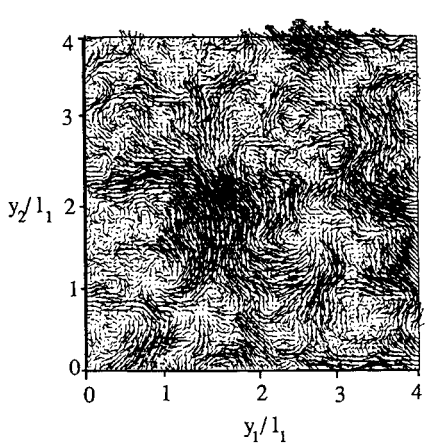

Fig. 3 Spatial distribution of the simulated turbulent velocity field at a given time; velocity vector is plotted in the plane y_1,y_2; and $K = 1714$ m^2/s^2, $\epsilon = 44.8 \times 10^6$ m^2/s^3, and $l_1 = 8.6 \times 10^{-4}$ m.

Table 1 Values of x/D which verify the three conditions of Fuchs for different values of the Strouhal numbers St

St (u_{ij} m/s)	x/D 1st condition	2nd condition	3rd condition
0.23 (125)	**12.1**	**12.0**	0.2
3.0 (125)	0.9	**12.0**	2.7
0.23 (300)	5.0	**12.0**	0.5
3.0 (300)	0.4	**12.0**	**6.8**

In a plane containing the jet axis, the source domain is divided in patches of area $l_1 \times l_2$. In practice, the K-ϵ closure provides very close estimates of l_1 and l_2. As a consequence, the source domains are square and have a typical size l_1. In any event, the result of the simulation is not sensitive to the exact size attributed to each source domain.

4) The turbulent velocity field is generated in this step. One assumes a homogeneous turbulence in each square source domain, and one applies a stochastic method to synthesize the turbulent field. For each source domain, and after a computation of the random field, one calculates the turbulent velocity at all of the points using Eq. (13). In a second step and for each point belonging to the given source domain, the velocity time series are filtered numerically. The mean values of K and ϵ are utilized to define the filter transfer function $\tilde{H}(f)$ and, by a Fourier transform, the corresponding impulse response.

Figure 3 shows a realization of the random turbulent velocity field in a square domain of area $4l_1 \times 4l_1$. Several eddies of size l_1 are visible in this plot.

5) The source terms forming the right-hand side of Eq. (11) are calculated in this step. The mean flow velocity U_i and the generated turbulent velocity field u_{ti} are used to determine the three noise source terms of Eq. (11). The spatial differentiations of u_{ti} are directly deduced from Eq. (13).

6) In this step the propagation equations are solved. These equations have the linearized Euler form of Eqs. (10) and (11). The solution therefore accounts for effects of convection and refraction by the mean flow. It is obtained with the Eole code,[33] developed by the Département Acoustique et Mécanique Vibratoire of the Direction des Etudes et Recherches d'Electricité de France. The source terms appearing on the right-hand side of Eq. (11) are determined as indicated in the previous steps.

The method used in Eole is based on a fractional step scheme and relies on solutions of one-dimensional problems in terms of a weak formulation.[32] This is achieved with time-dependent test functions. The formulation leads to a solution of tridiagonal systems for each direction of propagation. The Courant number is kept at less than unity to obtain an accurate solution.

Theoretical analysis and numerical tests indicate that wave propagation is calculated with little dispersion and dissipation. Some applications to the propagation in hot jets show that the effects of convection and refraction appear clearly in the results.[33] As indicated in the Introduction, it is difficult to carry propagation calculations in three dimensions. For this reason we use an axisymmetric version of the code. This reduces the computational requirements, but it also implies that the noise sources in the jet have an azimuthal coherence. In turn, this introduces a directivity factor which will modify the spatial distribution of acoustic energy.

Numerical results obtained in this way for the acoustic pressure and velocity are compared in the next section with experimental data.

V. Validation of the Stochastic Noise Generation and Radiation Model

The SNGR model is now applied to the case of free turbulent jets. As a first validation, we study the directivity of the acoustic intensity $I(x,\theta)$. This intensity has been measured by Lush[26] in the far field at a distance $x = 120D$ where D is the exit diameter. In particular, we will verify that directivity

effects associated with refraction are correctly predicted in the downstream direction. The second validation consists of checking the spectrum of the acoustic power at two angular positions: $\theta = 15$ and $\theta = 90$ deg.

The tests are carried out for two jet configurations ($U_1 = 125$ m/s and 300 m/s). The wave propagation step is effected with the axisymmetric version of Eole.[33] Each source point represents an annular set of points which are subjected to the same turbulent fluctuations.

Choice of Step and Dimensions of the Mesh

To compare the numerical results with experimental data of Lush, one needs a domain of area $120D \times 120D$. In theory, the Eole code provides solutions to the far field since the set of Eqs. (10) and (11) govern the acoustic propagation in a medium at rest. However, a practical problem arises. If one wishes to propagate a signal of frequency 36 kHz (e.g., a Strouhal number equal to 3 for an initial velocity $U_1 = 300$ m/s), one must choose a mesh size Δy_1 of the order of 1.56 mm (a size which corresponds to six points per wavelength). A total mesh of 1923×1923 points would be required to reach $120D$ (for $D = 25$ mm) and a memory size of 693 megawords would be necessary for the numerical calculation. This is, for the moment, beyond the computer resources available to us. It is more appropriate to choose a maximum frequency which determines the mesh size and then select the computational domain size which is sufficient to obtain the far-field radiation.

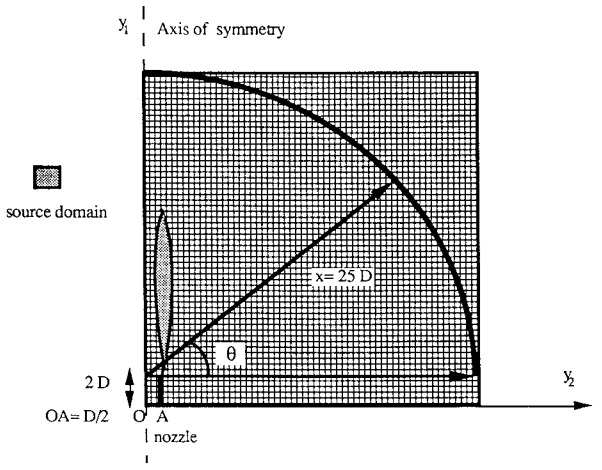

Fig. 4 Schematic representation of the computational domain.

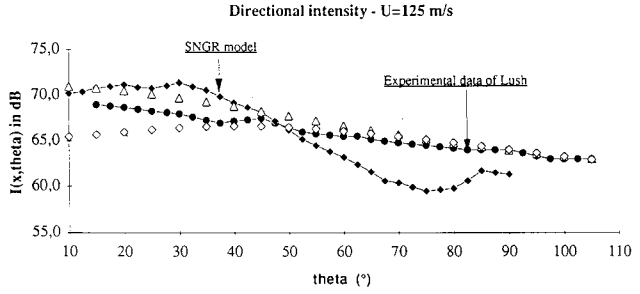

a) $U_1 = 125$ m/s

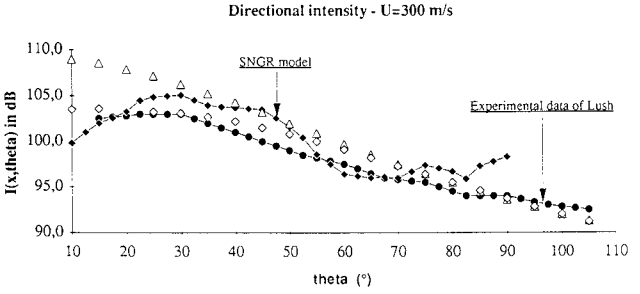

b) $U_1 = 300$ m/s

Fig. 5 Directional intensity $I(x,\theta)$ plotted as a function of the observation angle θ; intensity is given in dB, Ref. 10^{-12} W/m^2: • experimental data of Lush, ◆ SNGR model, △ Ribner model, and ◇ Goldstein model.

Three conditions stated by Fuchs[34] define the far field. If x designates the distance required to be in the far field, one should have

$$x/\lambda >> 1 \tag{23}$$

where λ is the wavelength. To be in the geometric far field,

$$x/l_s >> 1 \tag{24}$$

where l_s is a typical length of the acoustic source domain. The typical size of source region l_s is order of $12D$ (Ref. 11).

To assure that the directivity of acoustic intensity is independent of x,

$$x/l >> l/\lambda \tag{25}$$

where l is a characteristic turbulent scale. From the experimental data of Davies et al.,[35] $l = 0.13y_1$ (y_1 designates the axial distance from the nozzle exhaust).

If one limits the Strouhal number St to the range 0.23–3.00, some of the acoustic radiation will not be described. However, one may show (see, for example, Béchara et al.[11]) that about 90% of the power radiated by the jet belongs to this frequency range. Table 1 gives the values x/D which satisfy the three conditions (23–25). This table shows that the ratio x/D must be greater than 12. As the maximum memory size accessible to us corresponds to a grid of 400×400 points (in our case with Eole) and the elementary grid size Δy_1 corresponding to the Strouhal number 3.0 is equal to 1.56 mm, the grid dimensions are $25D \times 25D$ (and the ratio x/D is equal to 25). However, one notices that the length of the source domain in the y_2 direction is of order of $1D$ (Fig. 4). Thus, for the points situated on the circle of radius $x = 25D$ and near the y_1 axis, the second condition yields the required ratio $x/D >> 1$. Finally, with the exception of points near the jet axis, in the low-frequency range and for the first flow configuration (jet velocity $U_1 = 125$ m/s), Table 1 shows that the acoustic far-field hypothesis is verified for $x = 25D$.

Directivity of the Acoustic Intensity

Assuming that the far field is obtained on a circle centered at the nozzle and taking a radius $x = 25D$, the directional acoustic intensity is given by

$$I(x,\theta) = \frac{\overline{p_a^2}}{\rho_0 c_0} \tag{26}$$

The mean time average computation is carried out over a time interval which is at least three periods long for the lowest frequency $St = 0.23$. To compare these calculations with the results of Lush, it is necessary to account for the square of the distance ratio ($25D/120D$).

The directional acoustic intensity $I(x,\theta)$ calculated for the two velocities 125 m/s and 300 m/s show that the SNGR model overestimates the data of Lush by about 50 dB at 125 m/s and by 30 dB at 300 m/s. One may recall at this point that the synthetic turbulent field contains two types of fluctuations: the first type does not produce propagating components, and only generates pseudosound. The second type of fluctuations generates acoustic waves which propagate to the far field. Thus, it appears that the acoustic level deduced with the model is overestimated because it contains a pseudosound

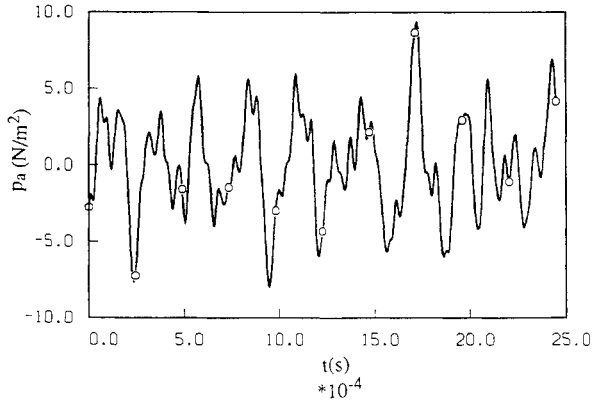

a) $\theta = 15$ deg

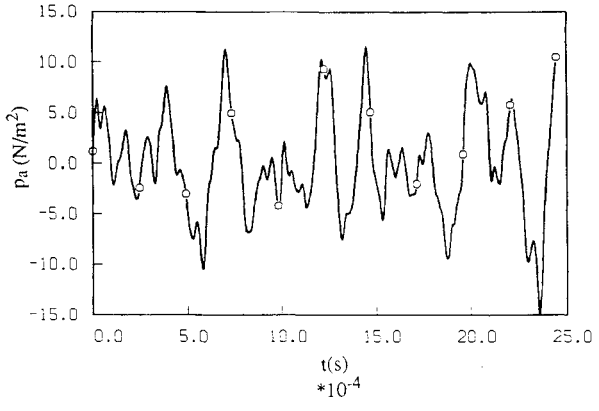

b) $\theta = 90$ deg

Fig. 6 ○, temporal evolution of the acoustical pressure for U_1 = 300 m/s.

component. It is then natural to identify and extract the propagative part of the turbulent fluctuations of the synthesized velocity before calculating the wave propagation with the Eole code.

To solve this identification problem, one may use the work of Ffowcs Williams[5], who shows that the turbulent structures characterized by their wave number k and angular frequency, radiate noise, if the modulus of k is equal to ω/c_0. If one then identifies the characteristic frequency of turbulence in each subdomain with $f_0 = \epsilon/K$, the corresponding spatial wave number will be $k_s = 2\pi\epsilon/(Kc_0)$ and the associated turbulent energy takes the form $\sqrt{E(k_s)\Delta k_s}$. In the modal sum (13) used to simulate the turbulent flow, one selects a single mode corresponding to the wave number k_s obtained by applying this selection rule over all of the subdomains. The numerical calculations carried out for 125 and 300 m/s show that one correctly predicts the acoustic level in the two cases, see Figs. 5a and 5b. These figures also show predictions obtained with the Ribner and Goldstein source models. The calculations based on these models are explained in a companion paper.[11] All of the statistical quantities which are involved in the model are deduced from calculations of a turbulent jet using a turbulence closure model. Comparison of the predictive capabilities of the three models is left to the reader. Of the three, only the SNGR model allows for refraction effects. One finds that the SNGR model correctly determines the attenuation of sound emission due to refraction. However, the magnitude of the predicted attenuation at low angles of observation ($\theta < 15$ deg) is greater than that found in experiments, because convective effects which compensate the refraction effect are not well-accounted for by the present source model. For angles close to 90 deg, one finds an increase in the acoustic level. This behavior is due to the proximity of the boundary which is not treated as a perfectly absorbing one by the numerical procedure. One also notices in this figure the influence of computational domain size on the directivity at angles which are too close to 0 deg. To explain this point, one may recall that the second condition of Fuchs on the geometrical aspect is less well-satisfied because the source occupies about a half of the computational domain.

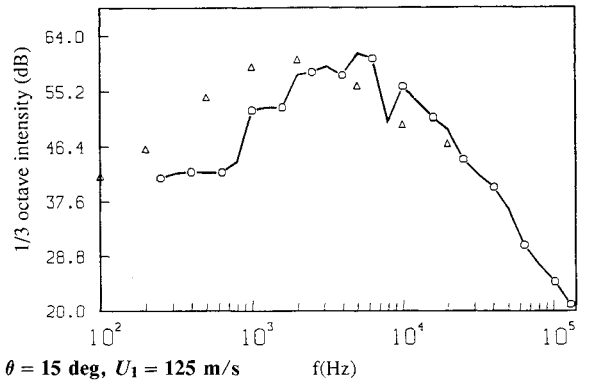

a) $\theta = 15$ deg, $U_1 = 125$ m/s

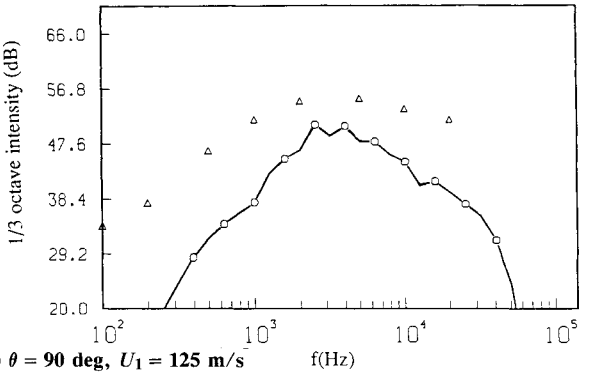

b) $\theta = 90$ deg, $U_1 = 125$ m/s

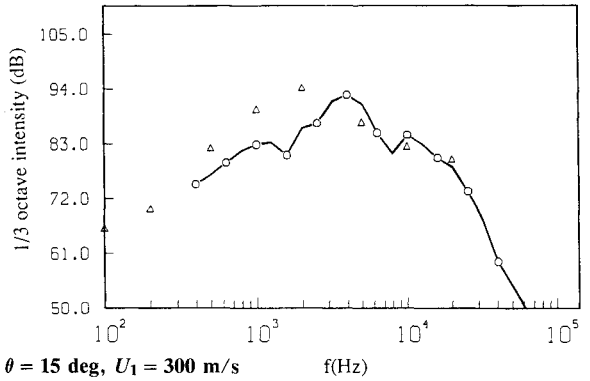

c) $\theta = 15$ deg, $U_1 = 300$ m/s

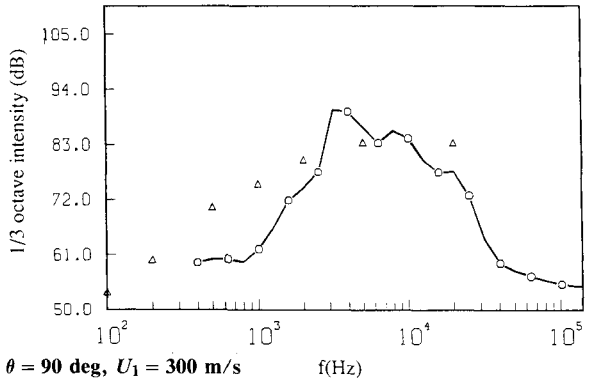

d) $\theta = 90$ deg, $U_1 = 300$ m/s

Fig. 7 Acoustical intensity spectrum ⅓ octave band distribution and comparison with the data of Lush: ○, SNGR model and △, experimental data of Lush.

Acoustical Intensity Spectrum

To verify the spectral content of the acoustic intensity calculated with the SNGR model, we now examine the computed power spectral densities with the measured spectra reported by Lush[26] for $\theta = 15$ and 90 deg for the two velocities 125 and 300 m/s. Figures 6a and 6b display the temporal evolution of the acoustic pressure signal obtained at one point for a nominal velocity $U_1 = 300$ m/s. The signal generated by the model resembles that recorded in experiments. A third octave spectrum calculated in the four cases is plotted in Figs. 7a–7d along with experimental spectra for comparison. Note that for frequencies which are less than 1500 Hz the numerical spectra underestimate the values found by Lush especially at $U_1 = 125$ m/s. This underestimation is partly due to the reduced number of samples obtained from the calculations, which does not allow an averaging over a sufficient time period. In practice, the time step is imposed by the computational requirements associated with a high-frequency propagation. There is also a CPU time limit that we cannot exceed. These two constraints determine the amount of time samples available.

VI. Concluding Remarks

In this article we devise a new stochastic SNGR model for noise generation and radiation from the turbulent flowfield. The modeling consists of extending the linearized Euler equations of propagation to the treatment of noise generation. Source terms of noise due to turbulence-turbulence and turbulence-flow interactions are identified and modeled from a knowledge of the mean flow in combination with a stochastic simulation of the turbulent velocity. Spatial and temporal scales are imposed on this simulation to obtain a realistic space-time series. The SNGR model is developed and tested in the case of free turbulent jets and the numerical results are compared with the experiments of Lush. The results obtained are quite encouraging. The model allows a qualitative estimation of the directional acoustic intensity and of its spectral content. To calculate the acoustic level, we assume that only one part of the turbulence contributes to the acoustic emission, precisely, the turbulent structures characterized by a wave number modulus k equal to ω/c_0. In addition, the SNGR model allows an estimation of the sound refraction at angles close to the jet axis, an effect which is especially important at high velocities.

Comparisons between our calculations and experiments of Lush indicate that the modeling strategy has a predictive potential. Of course, the model requires a range of assumptions, and we are aware that the choices made are not unique. There are two important limitations of the present implementation. First, the convective features of the turbulent fluctuations are not represented in the model and, consequently, the convective amplification that is typical of moving noise sources is not retrieved. In addition, the propagation is treated with an axisymmetric code, and this modifies the spatial radiation from the sources. It would be easy to introduce convective features by simply moving the fluctuations in each source volume with a given convection velocity. It will be more difficult to use a three-dimensional propagation scheme because of current computer limitations. However, one may note that the numerical codes used to calculate the flow and the wave propagation are not specific to jet configurations and, hence, the SNGR model could be applied to more complex flows. In this case, where the analytical solutions are difficult to derive, this model can be employed to perform parametric studies.

Acknowlegments

We wish to express our grateful thanks to Pascal Esposito and Jean-Luc Trollé for many helpful discussions. Suggestions made by the reviewers have helped us greatly.

References

[1]Lighthill, M. J., "On Sound Generated Aerodynamically—I. General Theory," *Proceedings of the Royal Society of London*, Vol. 211, Ser. A, No. 1107, 1952, pp. 564–587.

[2]Ribner, H. S., *The Generation of Sound by Turbulent Jets*, Academic Press, New York, 1964, pp. 103–182.

[3]Ribner, H. S., "Quadrupole Correlations Governing the Pattern of Jet Noise," *Journal of Fluid Mechanics*, Vol. 38, No. 1, 1969, pp. 1–24.

[4]Ribner, H. S., "On the Role of the Shear Term in Jet Noise," *Journal of Sound and Vibration*, Vol. 52, No. 1, 1977, pp. 121–132.

[5]Ffowcs Williams, J. E., "The Noise from Turbulence Convected at High Speed," *Philosophical Transactions of the Royal Society of London*, Vol. 225, Ser. A, No. 1061, 1963, pp. 469–503.

[6]Crighton, D., "Basic Principles of Aerodynamic Noise Generation," *Progress in Aerospace Science*, Vol. 16, No. 1, 1975, pp. 31–96.

[7]Goldstein, M. E., and Rosenbaum, B., "Effect of Anisotropic Turbulence on Aerodynamic Noise," *Journal of the Acoustical Society of America*, Vol. 54, No. 3, 1973, pp. 630–645.

[8]Goldstein, M. E., *Aeroacoustics*, McGraw-Hill, New York, 1976, Chap. 2.

[9]Ribner, H. S., "Perspectives in Jet Noise," *AIAA Journal*, Vol. 19, No. 12, 1981, pp. 1513–1526.

[10]Pao, S. P., and Lowson, M. V., "Some Applications of Jet Noise Theory," 8th Aerospace Sciences Meeting, AIAA Paper 70-233, New York, Jan. 1970.

[11]Béchara, W., Lafon, P., and Candel, S., "Application of a k-ϵ Model to the Prediction of Noise for Simple and Coaxial Free Jets," *Journal of the Acoustical Society of America* (submitted for publication).

[12]Béchara, W., "Modélisation du bruit d'écoulements turbulents libres," Thèse de Doctorat, Ecole Centrale Paris, France, No. 1992-02, 1992.

[13]Phillips, O. M., "On the Generation of Sound by Supersonic Turbulent Shear Layers," *Journal of Fluid Mechanics*, Vol. 9, No. 1, 1960, pp. 1–28.

[14]Mani, R., "The Influence of Jet Flow on Jet Noise. Part I: The Noise of Unheated Jets," *Journal of Fluid Mechanics*, Vol. 73, No. 4, 1976, pp. 753–778.

[15]Lilley, G. M., "The Generation and Radiation of Supersonic Jet Noise. Vol. IV—Theory of Turbulence Generated Jet Noise, Noise Radiation from Upstream Sources, and Combustion Noise, Part II: Generation of Sound in a Mixing Region," Air Force Aero Propulsion Lab., AFAPL-TR-72-53, July 1972.

[16]Berman, C., "Noise from Non-Uniform Turbulent Flows," 12th Aerospace Sciences Meeting, AIAA Paper 74-2, Washington, DC, Jan. 1974.

[17]Balsa, T. F., "The Far Field of High Frequency Convected Singularities in Sheared Flows, with an Application to Jet Noise Prediction," *Journal of Fluid Mechanics*, Vol. 74, No. 2, 1976, pp. 193–208.

[18]Goldstein, M. E., "High Frequency Sound Emission from Moving Point Multipole Sources Embedded in Arbitrary Transversally Sheared Mean Flows," *Journal of Sound and Vibration*, Vol. 80, No. 4, 1982, pp. 499–522.

[19]Goldstein, M. E., "The Low Frequency Sound from Monopole Sources in Axisymmetric Shear Flows, with Application to Jet Noise," *Journal of Fluid Mechanics*, Vol. 70, No. 3, 1975, pp. 595–604.

[20]Balsa, T. F., "The Acoustic Field of Sources in Shear Flow with Application to Jet Noise: Convective Amplification," *Journal of Fluid Mechanics*, Vol. 79, No. 1, 1977, pp. 33–47.

[21]Schubert, L. K., "Numerical Study of Sound Refraction by a Jet Flow: I. Ray Acoustics," *Journal of the Acoustical Society of America*, Vol. 51, No. 2, 1972, pp. 439–446.

[22]Schubert, L. K., "Numerical Study of Sound Refraction by a Jet Flow: II. Wave Acoustics," *Journal of the Acoustical Society of America*, Vol. 51, No. 2, 1972, pp. 447–463.

[23]Candel, S. M., "Numerical Solution of Conservation Equations Arising in Linear Wave Theory: Application to Aeroacoustics," *Journal of Fluid Mechanics*, Vol. 83, Dec. 1977, pp. 465–493.

[24]Candel, S. M., and Crance, C., "Direct Fourier Synthesis of Waves: Application to Acoustic Source Radiation," *AIAA Journal*, Vol. 19, No. 3, 1981, pp. 290–295.

[25]Berman, C., and Ramos, J., "Simultaneous Computation of Jet Turbulence and Noise," 12th Aeroacoustics Conf., AIAA Paper 89-1091, San Antonio, TX, April 1989.

[26]Lush, P. A., "Measurements of Subsonic Jet Noise and Comparison with Theory," *Journal of Fluid Mechanics*, Vol. 46, No. 3, 1971, pp. 477–500.

[27]Kraichnan, R. H., "Diffusion by a Random Velocity Field," *The Physics of Fluids*, Vol. 13, No. 1, 1970, pp. 22–31.

[28]Karweit, M., Blanc-Benon, P., Juvé, D., and Comte-Bellot, G.,

"Simulation of the Propagation of an Acoustic Wave Through a Turbulent Velocity Field," 17th International Union of Theoretical and Applied Mechanics, Grenoble, France, Aug. 1988, pp. 21–27.

[29]Karweit, M., Blanc-Benon, P., Juvé, D., and Comte-Bellot, G., "Simulation of the Propagation of an Acoustic Wave Through a Turbulent Velocity Field: A Study of Phase Variance," *Journal of the Acoustical Society of America*, Vol. 89, No. 1, 1991, pp. 52–62.

[30]Hinze, J. O., *Turbulence*, 2nd ed., McGraw-Hill, New York, 1975, Chap. 3.

[31]Laurence, D., "Code Ulysse: Note de principe," Direction des Etudes et Recherches d'Electricité de France, HE-41/89-33B, April 1989.

[32]Esposito, P., "A New Numerical Method for Wave Propagation in a Complex Flow," 5th International Conf. on Numerical Methods in Laminar and Turbulent Flow, Montréal, Canada, July 1987.

[33]Lafon, P., "Propagation acoustique bidimensionnelle. Deux applications du code EOLE," Direction des Etudes et Recherches d'Electricité de France, HP 54/89.010, Feb. 1989.

[34]Fuchs, H. V., "On the Application of Acoustic Mirror, Telescope and Polar Correlation Techniques to Jet Noise Source Location," *Journal of Sound and Vibration*, Vol. 58, No. 1, 1978, pp. 117–126.

[35]Davies, P. O. A. L., Fisher, M. J., and Barratt, M. J., "The Characteristics of the Turbulence in the Mixing Region of a Round Jet," *Journal of Fluid Mechanics*, Vol. 15, No. 3, 1963, pp. 337–367.